Published in Paleoceanography 18/1 : 15 (1-14), 2003,
which should be used for any reference to this work

Sedimentary phosphorus record from the Oman margin: New evidence of high productivity during glacial periods

Federica Tamburini,[1] Karl B. Föllmi, and Thierry Adatte
Institut de Géologie, Université de Neuchâtel, Neuchâtel, Switzerland

Stefano M. Bernasconi
Geologisches Institut, Eidgenossische Technische Hochschule-Zentrum, Zürich, Switzerland

Philipp Steinmann
Institut de Géologie, Université de Neuchâtel, Neuchâtel, Switzerland

[1] The northern region of the Arabian Sea is one of the biologically most fertile regions of the world oceans, with present productivity rates varying between 150 and 2500 mgC/m^2 × day [*Madhupratap et al.*, 1996]. This is related to the influence of the southwesterly summer monsoon which causes vigorous upwelling along the Oman margin. Upwelling ceases during northeasterly winter monsoon activity; productivity rates, however, remain relatively high (about 800 mgC/m^2 × day), related to deep water mixing [*Madhupratap et al.*, 1996]. The goal of this study is to verify if during the last glacial period, a period in which winter monsoon conditions prevailed, productivity rates were similarly high. With an analysis of phosphorus phases, stable nitrogen isotopes, organic matter content, and bulk mineralogy of the upper 10 m of the cores of ODP Hole 724C (corresponding to the last 140,000 years, sample resolution is ∼5 kyr), we provide new evidence of high productivity during this last glacial period (marine isotopic stages 2, 3, and 4). This was probably related to the combined effect of (1) increased eolian input of iron-containing dust due to dryness on the adjacent continent and stronger winter monsoon, and (2) regeneration and diffusion of dissolved phosphorus from the sediments to the water column due to variations in the position and intensity of the Oxygen Minimum Zone. These findings suggest that there is no one-to-one relationship between summer monsoon activity and productivity, which emerges to be a quasi-persistent phenomenon across glacial and interglacial stages. *INDEX TERMS:* 4267 Oceanography: General: Paleoceanography; 4805 Oceanography: Biological and Chemical: Biogeochemical cycles (1615); 4845 Oceanography: Biological and Chemical: Nutrients and nutrient cycling; 4851 Oceanography: Biological and Chemical: Oxidation/reduction reactions; *KEYWORDS:* phosphorus, Oman margin, monsoon, productivity

1. Introduction

[2] Modern and ancient upwelling regions have been shown to have an impact on the carbon cycle [*Heinze et al.*, 1991; *Raymo*, 1994; *Goddéris and François*, 1995], and thus on climate. Estimates of global primary production in oceans indicate that the contribution of upwelling regions amounts to 4.8 Gt C/year, representing 67% of total new production [*Chavez and Toggweiler*, 1995]. New production supplied by monsoon-related upwelling regions (1.5% of world's ocean surface) represents about 5.5% (0.4 Gt C/year) of global primary production.

[3] The Oman margin is located south of the Arabian peninsula and constitutes the northwestern side of the Arabian Sea (Figure 1). This region is influenced by the Indian Ocean Monsoon, which is characterized by a seasonal reversal of the winds, coupled with an alternation of dry and wet conditions on the mainland [*Webster et al.*, 1998]. Intermediate waters along the Oman margin are mainly formed by the outflow of warm, O_2-depleted and nutrient-rich waters from the Red Sea, while contributions from the Persian Gulf mostly influence shallower waters (<300 m). The extent of these outflows is controlled by monsoon intensity, with winter-summer changes in wind direction affecting the amount of nutrients (P and N) exported to the Indian Ocean [*Bethoux*, 1988].

[4] During summer monsoon, which dominates during full interglacial periods, in response to the injection of nutrients from below the thermocline, modern primary productivity in surface waters averages >500 mgC/m^2 ×

[1]Now at Woods Hole Oceanographic Institution, Marine Chemistry and Geochemistry, Woods Hole, Massachusetts, USA.

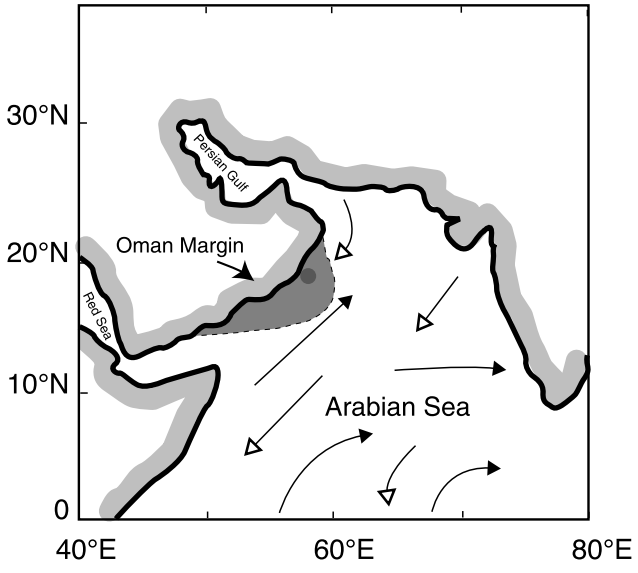

Figure 1. ODP Site 724 location in the Oman margin (dot). The Oman margin upwelling area is marked in light gray and arrows show wind directions during summer (solid) and winter monsoon (open).

day between May and October, but drops to about 150 mgC/m^2 × day during the rest of the year (according to *Prell and Niitsuma* [1989], but see below). Stratification of the water masses, sluggish circulation and decomposition of organic matter produce an Oxygen Minimum Zone (OMZ) between 200 and 1200 m, with O_2 concentrations below 0.2 ml/l [*Prell et al.*, 1989].

[5] During winter monsoon, arid conditions prevail on the mainland and northeasterlies become predominant, resulting in onshore Ekman transport, which stops upwelling activity [*Prell*, 1984; *Webster et al.*, 1998; *Altabet et al.*, 1999]. This situation is assumed to be dominating during glacial periods [*Burns et al.*, 1998].

[6] Summer monsoon-induced upwelling, however, may not be the only factor promoting high productivity along the coasts of the Arabian Sea [*Weedon and Shimmield*, 1991]. Reconstructed Sea Surface Temperature (SST) and organic carbon content variations do not correlate with other monsoon proxies, such as *Globigerina bulloides* percentages [*Prell and Kutzbach*, 1987; *Prell et al.*, 1992]. These apparent contradictions have already been interpreted as evidence for regional mechanisms other than monsoon controlling nutrient supply and productivity during glacial times [*Anderson and Prell*, 1991; *Zahn and Pedersen*, 1991]. Moreover, recent observations of plankton variability in the northeastern Arabian Sea [*Madhupratap et al.*, 1996], indicate the occurrence of relatively high productivity, with a maximum of 807 mgC/m^2 × day, during winter (December–February). Dry winter monsoon promotes evaporation, cooling of surficial waters and consequent sinking. This winter deep water mixing down to 800 m [*Reichart et al.*, 1998] can concur in sustaining primary production during winter and, possibly, glacial periods [*Madhupratap et al.*, 1996]. Along with these processes, major changes in oceanic circulation linked to glacioeustatism, took place at glacial-interglacial transitions and influenced the hydrography of the region [*Kallel et al.*, 1988; *Zahn and Pedersen*, 1991].

[7] Here we present a multiproxy study on sediments from ODP Site 724 along the Oman margin. We have analyzed bulk mineralogy, organic matter, nitrogen stable isotopes, and characterized different forms of phosphorus in the sediments, in trying to decipher the role of the monsoon and its changes on productivity, and to search for mechanisms other than monsoon sustaining productivity at glacial-interglacial time scales in this area.

2. Material and Methods

[8] The data presented here are from ODP Leg 117, Hole 724C (Oman Margin, Figure 1). The age model used in this study is based on the isotopic stratigraphy provided by *Zahn and Pedersen* [1991]. Hole 724C (Oman Margin, 18°27.713′N, 57°47.147′E, 592.8 m water depth) was sampled from 0 to 10.27 mbsf, at a time resolution of about 5 kyr, yielding a total of 26 samples. These sediments consist of dark calcareous clayey silt, moderately bioturbated throughout, with abundant well-preserved nannofossils and foraminifers. The sedimentation rates for the studied sequence are relatively low and range between 4 and 17 cm/kyr. No evidence of redeposition and/or winnowing was detected [*Prell et al.*, 1989].

[9] All samples, of approximately 10 c^3 each, were oven-dried at 50°C and divided in subsamples. All analyses were performed at the GEA laboratory of the Geological Institute in Neuchâtel, except for ICP- AES and nitrogen stable isotope analyses.

[10] 5 g of dried sediment were ground to obtain a homogeneous powder with particle sizes <40 μm. An aliquot of this powder was pressed (20 bars) to determine bulk sediment mineralogy by XRD (SCINTAG XRD 2000 Diffractometer) based on a semi-quantitative estimation, and using external standards [*Kübler*, 1987]. The relative error of the bulk rock mineralogy is about 5% (RSD).

[11] The characterization of organic matter was performed on about 100 mg of dried and ground sediment, with a Rock-Eval 6, using the standard whole rock pyrolysis method [*Espitalié et al.*, 1986; *Lafargue et al.*, 1996].

[12] Nitrogen contents and stable isotopic analyses of the bulk sediment were performed at the Stable Isotope Laboratory, ETH-Zentrum, Zürich, using a Carlo Erba CNS2500 CHN Elemental Analyzer coupled with a FISONS OPTIMA mass spectrometer. Mean errors, calculated as the relative standard deviations on measurements are about 0.15‰. All data are reported in the conventional δ notation with respect to atmospheric nitrogen (AIR‰). Sample replicates have been analyzed to assess the validity of the data.

[13] Total nitrogen is here considered as representing the organic nitrogen content. To justify this assumption, our data were plotted on a TOC wt% versus Tot. N wt% diagram (Figure 2). The x-intercept of the calculated regression line has a negative value, indicating that when organic matter is lacking in the sediments, no significant inorganic component of nitrogen is present [*Hedges et al.*, 1988]. Therefore we have analyzed bulk sediment for $\delta^{15}N$ estimation, avoiding acidification of the sample, which

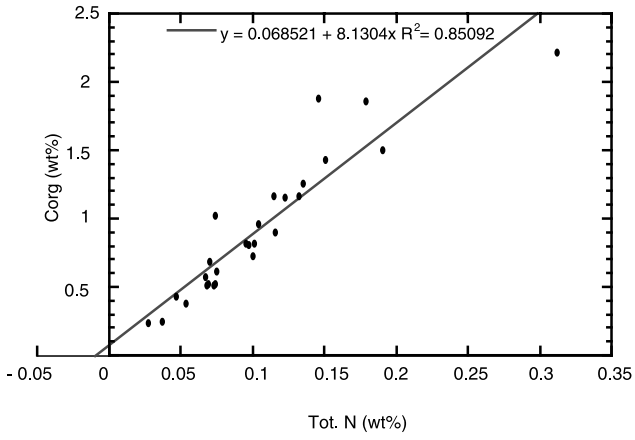

Figure 2. Correlation between C_{org} (wt%) and N_{tot} (wt%) from Site 724. The intercept of the regression line on the x axis when $C_{org} = 0$ is negative ($y = 0$, $x = -0.008$), indicating that no important inorganic nitrogen fraction is present. This finding has allowed to avoid acidification. Tests carried out on several samples treated with HCl at different concentrations (10 and 30%), show, indeed, that decarbonation using HCl has a strong and somehow unpredictable effect on nitrogen isotopes. Nitrogen isotopic signal of those samples shows a change ranging between 0.02 and 4.4‰, with no apparent relation to the strength of the acid.

seems to attack part of the organic matter, resulting in the loss of up to 50% of Tot. N [*Lohse et al.*, 2000].

[14] Because of all diagenetic processes which influence the regeneration and redistribution of dissolved and reactive P in the uppermost sediments [*Broecker and Peng*, 1982; *Froelich et al.*, 1982; *Ingall and Jahnke*, 1994; *Jarvis et al.*, 1994; *Krajewski et al.*, 1994; *Föllmi*, 1996; *Ruttenberg and Gõni*, 1997; *Slomp*, 1997], it is critical to distinguish between different phosphorus sedimentary phases. Therefore we have used a 4-step sequential extraction technique, adapted from the SEDEX method [*Ruttenberg*, 1992; *Anderson and Delaney*, 2000]. This method utilizes progressive dissolution of solid phases in four steps to extract P associated with well defined sedimentary components: (1) iron and manganese oxi-hydroxides and P loosely absorbed on mineral surfaces, (2) authigenic minerals (carbonate fluorapatite (CFA)) and phosphorus associated to fish debris, to calcium carbonate, and smectite, (3) detrital material, so phosphorus associated to igneous, methamorphic and sedimentary apatites, and (4) organic matter (Table 1) [*Ruttenberg*, 1992]. During the first step of this extraction, because of the reduction of Fe by dithionite and subsequent complexation by citrate, we are able to separate also ferric Fe, referred as $Fe_{(CBD)}$ (see Table 1).

[15] *Shimmield and Mowbray* [1991] analyzed major elements (e.g., Ti, Al, Ca, P, and Fe) of sediments from Site 724. Because these ratios are independent of accumulation rates, we will compare them to our mineralogical and geochemical data to improve our interpretation.

3. Results and Discussion

3.1. Mineralogy

[16] Calcite, phyllosilicates, quartz, and dolomite contents are shown in Figure 3. Detrital silicates, calculated as the sum of quartz, phyllosilicates, plagioclase and K-feldspar, account on average for 30% (around 40% during glacial periods), of the sediments of the Oman core (Figure 3; K-feldspar and plagioclase never exceed 5% of the detritic fraction and are not shown). This relatively high percentage compared to other sites drilled during Leg 117, is probably due to the proximity of the coast. Because of its higher abundance and mass accumulation rates (MAR; Figures 3 and 4) during arid periods (glacial stages 4 and 2, and stage 3), and due to the absence of major rivers, the detrital material is considered as predominantly eolian with only

Table 1. Sequential Extraction Technique Applied for Phosphorus Phases Determination[a]

Step Name	Treatments	P Component Isolated[b]	Errors,[c] %	Detection Limits[d]
Iron-bound P[e]	10 ml CBD solution (6 hours) (0.22 M sodium citrate, 0.11 M sodium bicarbonate 0.13 M sodium dithionite)	exchangeable or loosely sorbed P reducible or reactive iron-bound P	3–6	0.03
	10 ml 1M $MgCl_2$ (2 hours)	PLUS Ferric Fe		
	10 ml H_2O (2 hours)			
Authigenic P[f]	10 ml 1M Na-acetate buffered to pH 4 with acetic acid (5 hours)	carbonate fluorapatite (CFA)	2–7	0.025
	10 ml 1M $MgCl_2$ (2 hours)	biogenic hydroxyapatite		
	10 ml 1M $MgCl_2$ (2 hours)			
	10 ml H_2O (2 hours)			
Detrital P[f]	10 ml 1N HCl (16 hours)	detrital fluorapatite-bound P	3–5	0.003
Organic P[f]	1 ml 50% (w/v) $MgNO_3$, dry in low oven, ash at 500°C (2 hours)	organic-bound P	2–5	0.004
	10 ml 1N HCl (24 hours)			

[a]From *Ruttenberg* [1992] and *Anderson and Delaney* [2000].
[b]Concentrations of all phases are expressed in mg/g of sediment.
[c]Errors for each phase determination are considered as the relative standard deviation calculated on replicate analyses of consistency standards.
[d]Detection limits are considered as 3 times relative standard deviation calculated on replicate analyses of blank solutions.
[e]Iron-bound phosphorus and ferric Fe concentrations were measured using an OPTIMA 3000 Perkin Elmer ICP-AES, at the Laboratoire des Eaux et de l'Environnement in Peseux, Switzerland.
[f]The other phases were measured using a Perkin-Elmer UV/Vis spectrophotometer Lambda 10 with a 5-cm quartz cell. Sample solutions were diluted in distilled water and a color developing agent was added to the solution, following the ascorbic acid method for phosphates [*Eaton et al.*, 1995].

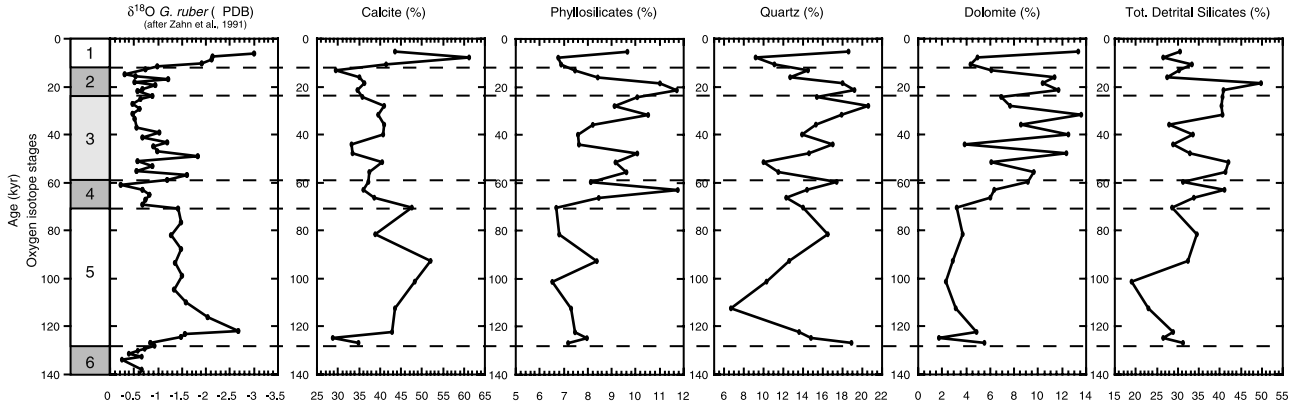

Figure 3. $\delta^{18}O$ data of *G. ruber* from Site 724 [*Zahn and Pedersen*, 1991]; percent of calcite, phyllosilicates, quartz, dolomite and total detrital silicates. Total detrital silicates percentage is calculated as the sum of quartz, phyllosilicates, plagioclase and K-feldspar. Horizontal lines represent the boundaries between isotopic stages [*Imbrie et al.*, 1984]. Glacial periods are represented in dark gray, while interglacial periods are represented in white. Stage 3, characterized by low insolation values and conditions intermediate between glacial and interglacial, is represented in light gray (see text for discussion).

minor fluvial contributions from the Arabian peninsula. During interglacial stage 5, both quartz and phyllosilicates show lower abundances (13% and 7% in average respectively) than during glacial stage 2 and stage 3 (15% and 9%). Prominent peaks are present at the end of stage 4 and during stage 2. Despite the similarity between general trends, the correlation between quartz and phyllosilicates is poor (r = 0.48), probably due to a different source of the material and/or to differentiation during transport.

[17] Detrital MAR (Figure 4) are low during interglacial 5 and show a 4-fold increase during glacial stages 4 and 2 and stage 3. The most prominent peak is observed during glacial stage 2, where it reaches about 104 mg/cm^2 $\times$ kyr. This observation confirms the correlation between land-derived and eolian-transported dust MAR with aridity [*Krissek and Clemens*, 1992], implying maximum dust transport during glacial times. The Ti/Al elemental ratio calculated for Site 724 [*Shimmield and Mowbray*, 1991] and interpreted as an indicator of aridity and a proxy of monsoon intensity, shows relatively higher values and higher variability during glacial periods, supporting the hypothesis of enhanced dust input deduced from our mineralogical data (Figures 3, 4 and 5).

[18] Dolomite shows the same trend as other detrital indices, with an increase to an average of about 9% during stages 4-2. The correlation with phyllosilicates is rather good (r = 0.64). The origin of dolomite is eolian, and its source area is the Northern Arabian Peninsula and Oman, where Permo-Triassic and Cretaceaous dolomitic series extensively outcrop [*Krissek and Clemens*, 1991; *Sirocko et al.*, 1993].

[19] The Oman margin sediments are characterized by high percentages (average of 40%) of mostly biogenic calcite (foraminifers and nannofossils are well preserved in the upper part of the sedimentary sequence) [*Prell and Niitsuma*, 1989], which resembles the general profile of the $\delta^{18}O$ record. Values are higher during interglacial stages 5 and 1, with peaks of about 50% at about 100 ka and 60%

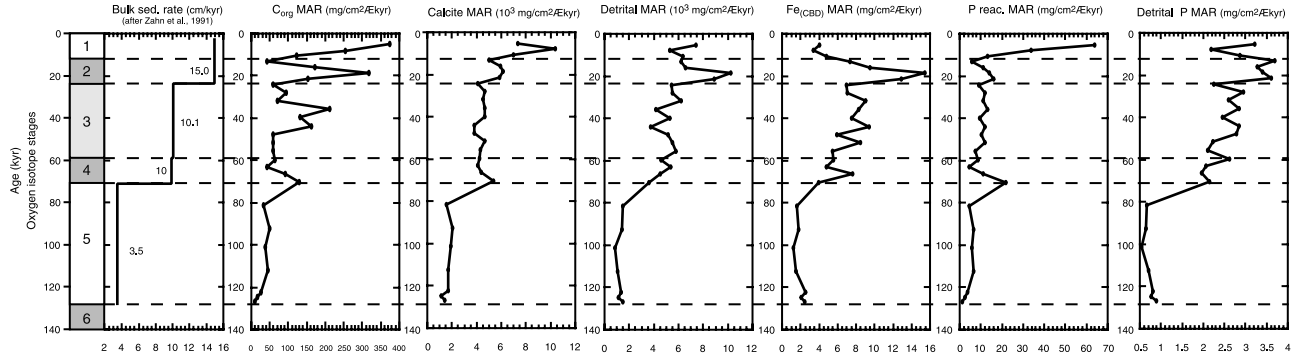

Figure 4. Bulk sedimentation rate (cm/kyr) from Site 724 [*Zahn and Pedersen*, 1991]; C_{org}, calcite, total detrital silicates, $Fe_{(CBD)}$, P_{reac}, and detrital P mass accumulation rates (MAR) from Site 724. Horizontal lines and isotopic stages are as in Figure 3.

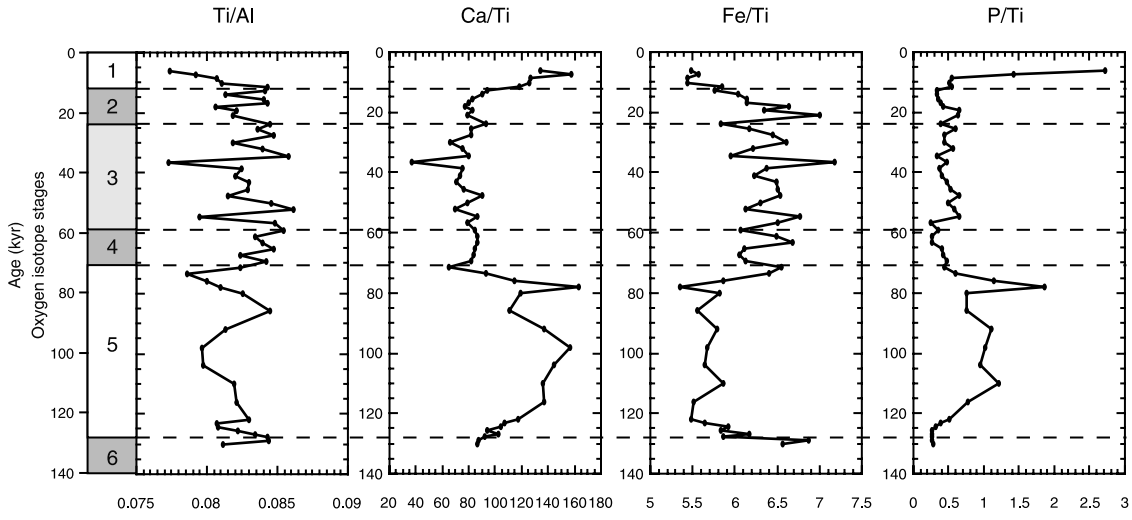

Figure 5. Major elemental ratios from Site 724 [*Shimmield and Mowbray*, 1991].

at 8 ka (Figure 3). The calcite record shows an upward-decreasing trend starting at about 90 ka, and reaches a minimum of about 30% at the top of stage 2.

[20] The relative importance of marine versus continental detrital input was higher during interglacial stages, as shown by the calcite record and the Ca/Ti curve (Figures 3 and 5) [*Shimmield and Mowbray*, 1991]. Variations in the calcite record probably stem from detrital dilution, and they may be interpreted as reflecting changes in aridity on the continent [*Weedon and Shimmield*, 1991]. Calcite MAR are, conversely, higher between stage 4 and 2 (Figure 4), possibly suggesting that a proportion of calcite is of detrital origin, as proposed by *Sirocko* [1989].

3.2. Phosphorus

[21] Phosphorus phases represent only a small fraction of the total sediment (about 0.1%), but relative variations between the phases are important. Authigenic phosphorus represents the most abundant form, on average 75% of total phosphorus, while detrital and Fe-bound phosphorus represent only 18% and 5% respectively (see Table 2 and Figures 6a and 7). The three reactive phases, Fe-bound, authigenic and organic-bound P, significantly increase after stage 2 and during the Holocene.

[22] Phosphorus extracted during the second step of the SEDEX method (see Table 1) mainly accounts for authigenic minerals, fish debris, and for P associated to smectite [*Ruttenberg*, 1992]. In all cases, as dissolved P is removed either from the water column or from the sediments prior to its association to these phases, we could consider and refer to them as authigenic.

[23] Biogenic calcium carbonate do not generally bear important quantities of P ($<3.2 \times 10^{-6}$ mg/g) [*Sherwood et al.*, 1987; *Delaney*, 1998] since phosphorus previously thought to be associated with carbonate shell debris, has been found to be principally bound to Fe-oxides coatings [*Sherwood et al.*, 1987]. Because smectite generally averages 12% of the clay fraction in the Oman margin sediments [*Debrabant et al.*, 1991], phosphorus bound to smectite accounts only for a minor proportion of the authigenic phase. Thus, the principal phases extracted during the second step of the SEDEX method are most likely to be authigenic Ca-apatite and fish debris. However, the SEDEX procedure does not allow to distinguish between these two components. *Schenau et al.* [2000], who employed a six-steps sequential extraction technique, estimated fish debris content in the Oman margin sediments to be more than 3 times lower than authigenic minerals. Sedimentary detrital apatite might also have been transported along with other detrital material to the Oman margin site. However, as phosphorus is generally tightly bound in the structure of sedimentary apatite [*Compton et al.*, 2000], it is most likely

Table 2. Mean Concentrations and Percentages of Phosphorus Phases From Site 724, Oman Margin[a]

	Fe-bound P, mg P/g sediment	Authigenic P, mg P/g sediment	Detrital P, mg P/g sediment	Organic-bound P, mg P/g sediment
Mean interglacial value	0.0719	1.3668	0.1761	0.0415
Mean glacial value	0.0523	0.8462	0.2134	0.0284
Minimum value	0.0410	0.2750	0.1290	0.0130
Average	0.0596	1.0390	0.2000	0.0330
Maximum value	0.1826	3.5820	0.2580	0.1500
P phases % on total P				
Interglacial average	4.34	82.52	10.63	2.51
Glacial average	4.59	74.21	18.71	2.49

[a]Differences between glacial and interglacial percentages are not significative for Fe- and organic-bound P. They are relatively important for detrital P and for authigenic P.

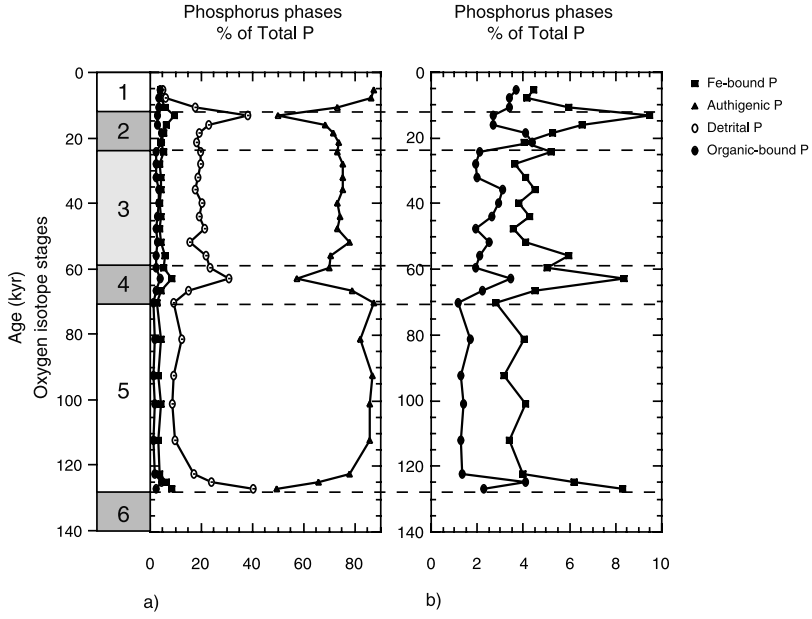

Figure 6. (a) Percent of total P in the analyzed phosphorus sedimentary phases. Authigenic and detrital P are the most abundant. (b) Fe-bound and organic-bound P show a down-core decreasing trend, while authigenic P is increasing, revealing a sink switch. However, these two phases may not explain alone the authigenic P increase (see text).

extracted during the third step of the SEDEX extraction (see below).

[24] Despite the lack of pore water analyses data, previous studies performed on cores from the Arabian Sea region support the hypothesis that most of the P extracted during the second step of the SEDEX method, is authigenic apatite. Recent studies on pore water and solid phases of phosphorus clearly indicate that phosphorite formation is an ongoing process in sediments around the Arabian Sea, and along the Oman margin [*Schenau et al.*, 2000]. Low pore water phosphate levels in the upper portion of Site 724 C (lower than 4 μmol PO_4/l) recorded onboard during Leg 117 were already interpreted as an indication of apatite precipitation [*Prell and Niitsuma*, 1989]. The relatively high P/Ti ratio values at Site 724 have also been explained as reflecting in-situ apatite precipitation [*Weedon and Shimmield*, 1991]. An indication of authigenic apatite precipitation is also given by the comparison between the percentages of the different phosphorus phases, which reveals a "sink switching" (Figure 6). The organic-bound P profile shows a down-core decreasing trend (Figure 6b), followed also by Fe-bound P. This trend is paralleled by the increase of authigenic P percentages (Figure 6a), indicating that this phase is forming at the expense of organic and Fe-bound P. The high con-

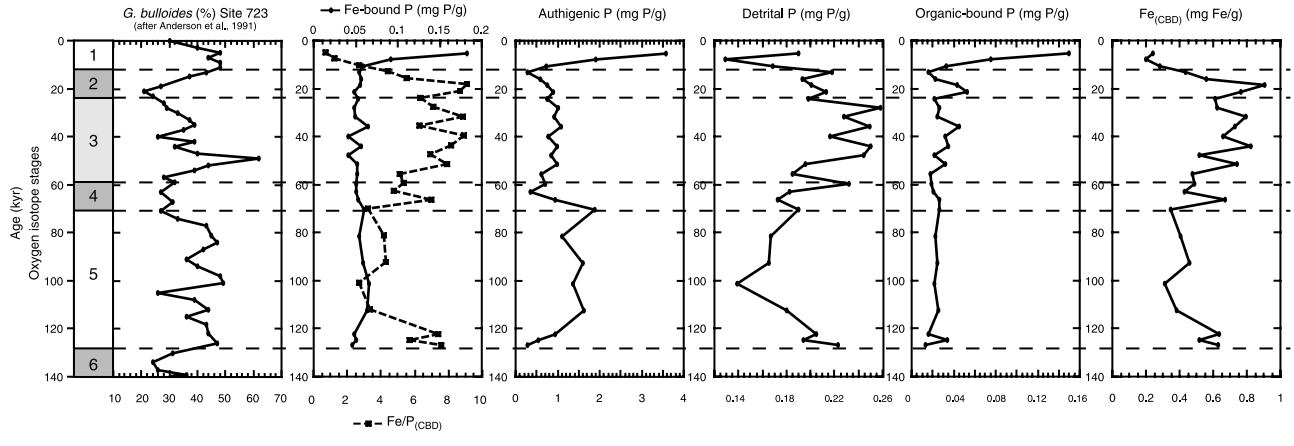

Figure 7. Percentage of *G. bulloides* from Site 723 [*Anderson and Prell*, 1991]; concentrations of Fe-bound P, authigenic P, detrital P, organic-bound P and $Fe_{(CBD)}$, from Site 724. The $Fe/P_{(CBD)}$ molar ratio is presented along with Fe-bound P. The different phases are defined in the text. Horizontal lines and isotopic stages are as in Figure 3.

centrations of the authigenic P recorded in the upper part of the core (Figure 6), and also found in nearby cores [*Schenau et al.*, 2000], might be explained by the presence of an F-poor and P-bearing authigenic mineral, representing the first step of Ca-apatite precipitation [*Krajewski et al.*, 1994].

[25] Authigenic phosphorus, which shows a remarkable correlation with the oxygen stable isotope and calcite records (r = 0.79 and 0.60 respectively), presents higher values during interglacial stages than during glacials. From average values of about 1.5 mg P/g during stage 5, it decreases to 0.3 mg P/g during stages 4 and 2, and averages 1 mg P/g during stage 3 (Table 2 and Figure 6). The P/Ti ratio at Site 724 [*Shimmield and Mowbray*, 1991], which correlates in trend with the authigenic P curve presented in this study (Figures 5 and 7), shows lower values during stages 4-2. Biogenic calcite (e.g., foraminiferal shells) may provide nucleation sites for CFA, and this could explain the good correlation between these two parameters. However, the presence of carbonatic sheels in sediments cannot account alone for apatite precipitation, as other chemical parameters are more important (e.g., phosphate and fluoride concentrations in porewater, alkalinity).

[26] Fe-bound P shows concentrations lower than 0.05 mg P/g, except in stage 1, when it reaches values up to 0.2 mg P/g (Figure 6). It is plausible that in the youngest samples, phosphorus extracted during the first step of the SEDEX method, accounts also for adsorbed P on clay and mineral surfaces (see Methods). In fact, during this interval, the Fe/$P_{(CBD)}$ ratio presents values close or even lower than 1 (Figure 7), suggesting that part of phosphorus extracted during this step clearly accounts for loosely sorbed phosphorus [*Ruttenberg*, 1992]. Ferric iron ($Fe_{(CBD)}$) follows the overall trend of detrital indices (r = 0.62 with detrital P), with a two-fold increase during stage 3 and glacial stage 2 compared to interglacial stages. Highest values are on the order of 0.8 mg Fe/g. Lack of correlation between $Fe_{(CBD)}$ and Fe-bound P (r = 0.46) may be due 1) to the nature of the Fe phases, and 2) to changes in environmental conditions at the sediment/water interface. The correlation between $Fe_{(CBD)}$ and other detrital parameters reflects the eolian origin of iron, and may suggest that iron is present in the sediments under a relatively well-crystallized form (i.e., goethite, hematite). These minerals, which are dissolved during the CBD step, constitute a less efficient sink for dissolved P than amorphous Fe oxyhydroxides [see *Slomp et al.*, 1996b]. Furthermore, the development of oxygen depleted conditions in the upper part of the sediments, might have reduced the thickness or even removed the oxidized sediment layer, and inhibit the adsorption of dissolved phosphorus by Fe-oxides [*Glenn*, 1990; *Slomp et al.*, 1996b]. *Sirocko et al.* [2000] provided geochemical evidences of extremely low oxygen levels, especially during the Last Glacial Maximum (LGM), along the Oman margin. *Lucotte et al.* [1994] used the Fe/$P_{(CBD)}$ ratio to infer paleoredox conditions in bottom waters and sediments from the Labrador Sea. At Site 724, this ratio shows the highest values during glacial periods (Figure 7), suggesting, indeed, low oxygen conditions [*Lucotte et al.*, 1994]. However, considered the detrital nature of Fe oxides, these values should be taken with caution.

[27] Detrital P (igneous, metamorphic, and sedimentary detrital apatite) is correlated to quartz (r = 0.65 and 0.67 during glacial times), with peaks during stages 4-2 of about 2.5 mg P/g and minima during interglacial stages 5 and 1. The lack of a strong correlation with other detrital indices such as phyllosilicates (r = 0.33), may indicate an alternate source for these detrital components. Detrital P MAR show the same trend of detrital silicates MAR, with higher values during stages 4-2, reaching maxima of about 3.5 mg/cm^2 $\times$ kyr during glacial stage 2 (Figure 4).

[28] Organic-bound P exhibits extremely low values, around 0.02 mg P/g, along the entire sequence and a sharp and pronounced increase at the beginning of stage 1. Higher variability is noticed during stage 3, and a more prominent spike, with values up to 0.05 mg P/g, is present at the beginning of stage 2.

[29] Reactive phosphorus percentages (the formerly biologically available phase, calculated as the arithmetic sum of Fe-bound, authigenic and organic-bound phosphorus) are lower during glacial periods, following the authigenic P trend, as this phase is the most abundant. This phase, in fact, diminishes about 10% during glacial periods (Figure 6). Total P, on the other hand, does not show important glacial-interglacial variations, but, as detrital P is not biologically available, it is questionable if total P might help in understanding the impact of changes in reactive P input on productivity.

[30] Reactive phosphorus MAR show a singular trend, compared to other proxies: values generally range between 10 and 15 mg/cm^2 $\times$ kyr, and they show no particular increasing trend due to higher sedimentation rates (Figure 4). Besides the Holocene increase of all the reactive phases of phosphorus, only two significant peaks are documented, at 70 ka and at 20 ka, both at the beginning of glacial periods. Otherwise it seems that reactive P fluxes to the sediments were fairly constant throughout the investigated period, unlike all the other measured parameters. $Fe_{(CBD)}$ MAR match the detrital MAR trend, with higher values during stages 4-2, and show a significant increase between 70 ka and 20 ka, where they reach values of 15 mg/cm^2 $\times$ kyr.

3.3. Organic Matter

[31] Immature marine organic matter is the primary component of organic material present at Site 724. This is suggested by the Tmax (Tmax = 420°C in average) and the hydrogen index (HI) values. HI values are generally higher than 150 mg HC/g total organic carbon (TOC), with few points above 400 mg HC/g TOC (Figure 8a). These data are in agreement with previous analyses [*Bertrand et al.*, 1991]. When Rock Eval analyses are performed on bulk sediments, as in this case, low values of HI could indicate a strong mineral matrix effect [*Espitalié et al.*, 1986]. The occurrence of a rock-matrix effect and the uniform origin of the organic matter are corroborated by the S_2 versus C_{org} graph (Figure 8b). The regression line in a S_2 versus C_{org} diagram should have a 0 intercept, if no mineral matrix is present, while a positive *x* axis intercept (as observed here, Figure 8b) generally indicates adsorption by minerals, with clays representing the main agent of adsorption [*Langford and Blanc-Valleron*, 1990]. The samples, linearly distrib-

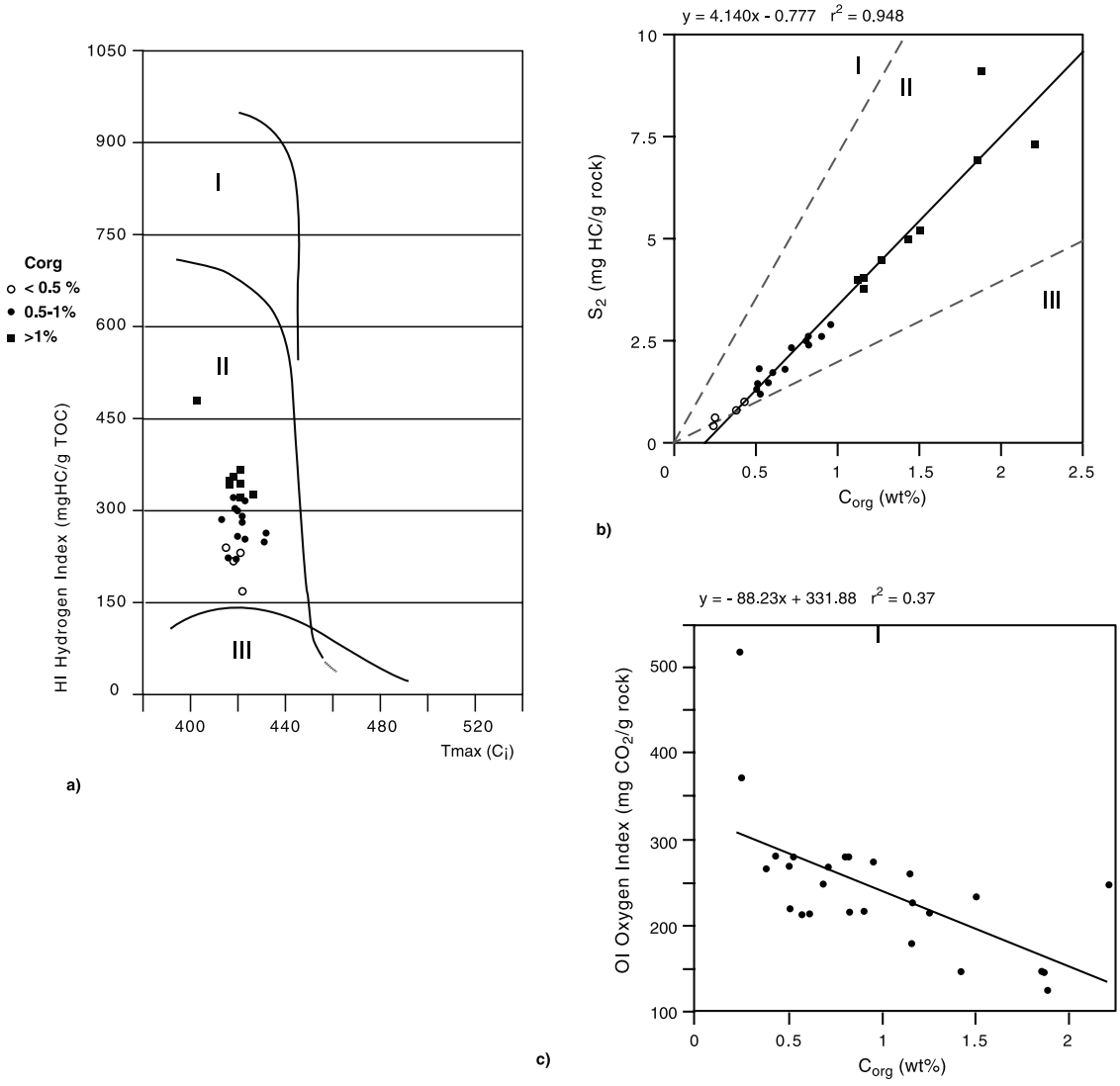

Figure 8. (a) HI versus T_{max} diagram. All the points, representing samples from Site 724, fall in the type II kerogen field (marine organic matter). (b) S_2 versus C_{org} diagram of the data from Site 724. Boundaries between the three fields are defined by *Langford et al*. [1990]. The slope of the regression line and the high degree of correlation confirm the marine origin of the organic matter. (c) C_{org} versus OI diagram. Samples with high organic matter content present low OI, indicating enhanced preservation due to deposition in a low oxygen environment.

uted, show a high correlation (r^2 = 0.95), indicating a coherent group. If the regression line is shifted towards the origin to eliminate the rock matrix effect [*Langford and Blanc-Valleron*, 1990], all the sample fall in the type II kerogen field, confirming the marine origin of the organic matter, with an average HI of 414, as given by the slope of the regression line.

[32] Average value of organic carbon from Site 724 is about 0.8 wt% (Figure 9), but the record exhibits large oscillations, especially during the last 60 kyr, with values up to 2 wt%. Higher organic carbon concentrations and accumulation rates are recorded during stage 3 and during glacial stage 2, with two major peaks between 30 and 45 ka and at 20 ka, during the LGM. High organic matter contents are also present in the Holocene part of the sequence.

[33] Organic carbon MAR show a high flux of organic matter during stage 3 and during glacial stage 2, while the lowest fluxes are recorded during interglacial 5. It is unclear if this trend is a real feature or represents the effect of higher glacial sedimentation rates (Figure 4) and consequent better preservation [*Canfield*, 1993]. The above relation was already observed by *Murray and Prell* [1991] for Site 722 on the Owen Ridge, but, despite their attempt of removing the possible effect of sedimentation rate, they found that greater fluxes of organic material were still related to glacial or winter-monsoon dominated periods [*Murray and Prell*, 1991]. Moreover, enhanced organic matter burial during

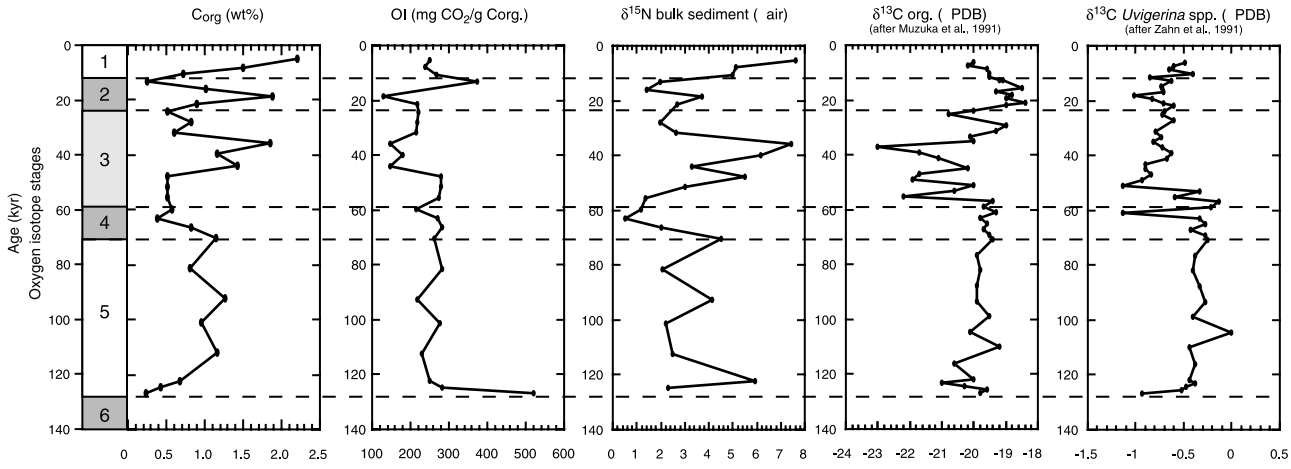

Figure 9. Concentration of Corg from Site 724; OI diagram, as determined by Rock Eval analysis; $\delta^{15}N$ of bulk sediment from Site 724; $\delta^{13}C_{org}$ [*Muzuka et al.*, 1991] and $\delta^{13}C$ *Uvigerina spp.* [*Zahn and Pedersen*, 1991] from Site 724. Horizontal lines and isotopic stages are as in Figure 3.

glacials (see peaks at 20 and at around 40 ka, Figure 4) correlates with low $\delta^{13}C$ *Uvigerina spp.* values (Figure 9), an endobenthic foraminifer, whose low carbon isotopic signature indicates higher supply and oxidation of organic matter in the sediments [*Zahn et al.*, 1986].

[34] $\delta^{15}N$ of the sediments shows a fairly good correlation ($r = 0.62$) with the organic carbon content: values are low during glacial stage 4 and the upper part of stage 2, with the lowest value of 1.2‰ reached during stage 4 (Figure 9); the two most prominent peaks are recorded during stage 3 ($\delta^{15}N = 7.4‰$), and at the top of the sequence, during the Holocene ($\delta^{15}N = 7.6‰$).

[35] The trend, maxima and minima of nitrogen isotopes of Site 724 sediments are in agreement with other nitrogen records, which are interpreted as indicating denitrification. $\delta^{15}N$ values from this study are generally lower than the values observed in nearby sites in the Oman region [*Altabet et al.*, 1999]. It is not clear why the magnitude of the signal (~6‰) is higher than the one observed by *Altabet et al.* [1999].

[36] The high degree of correlation between the $\delta^{15}N$ values and the organic matter content could, indeed, suggest the occurrence of denitrification, in situ or in remote areas. But the observed low values are difficult to decipher: one explication could be the influence of terrestrial organic matter, but evidences from other proxies (e.g., $\delta^{13}C$org, HI, C_{org}/N ratio, Figures 9 and 10) seem to exclude this possibility. Light interglacial $\delta^{15}N$ values have been already observed in sediments from other regions where denitrification is known to occur (i.e., the Cariaco Basin) [*Haug et al.*, 1998], and have been related to the imprint of nitrogen fixation by cyanobacteria, which lowered the nitrogen isotopic signal. Nitrogen fixation in the Indian Ocean and in the Red Sea is, indeed, an established phenomenon

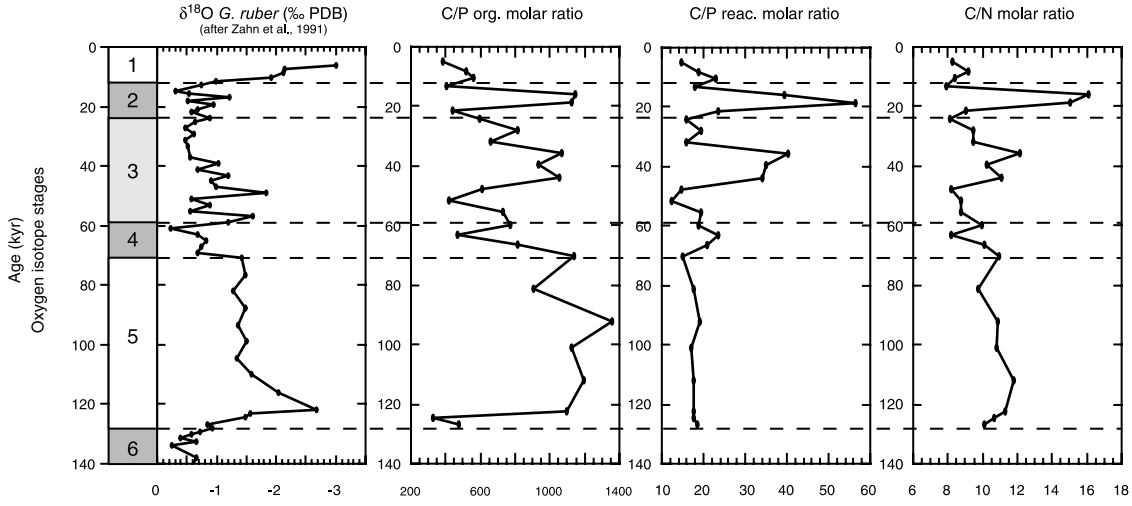

Figure 10. $\delta^{18}O$ data of *G. ruber* from Site 724 [*Zahn and Pedersen*, 1991]; C/P_{org}, C/P_{reac}, and C/N molar ratios, as defined in the text. Horizontal lines and isotopic stages are as in Figure 3.

[*Bethoux*, 1988; *Capone et al.*, 1997], which could have been fostered especially during glacial periods, when input of macronutrients and micronutrients (e.g., iron) was enhanced. So, generally low values are probably due to the imprint of nitrogen fixation, while relative changes may be attributed to different degree of denitrification.

[37] C/P_{org} and C_{org}/N elemental ratios are higher than the expected Redfield ratios for marine OM, indicating a strong depletion of P and a minor preferential loss of N during organic matter degradation (Figure 10). Again, these values could be explained by a larger input of terrestrial organic matter, but, as mentioned before, this is not supported by other data. Moreover, the lack of a positive correlation between light $\delta^{15}N$ and $\delta^{13}C$org data (interpolated from *Muzuka et al.* [1991]; see Figure 9) does not support this assumption.

[38] Relatively high elemental ratios in organic matter are thus considered as indicating organic material degraded in an oxygen-poor environment. The correlation of high C/P_{org} and C_{org}/N with lower OI (Figure 8c and 9), support this hypothesis [*Kenig et al.*, 1994].

[39] Organic matter is normally considered as the principal carrier of phosphorus to the sediment, and, once degraded, constitutes the major source of dissolved reactive phosphorus of the pore water. Thus, the elemental ratio between Corg and reactive P (C/P_{reac}) in Oman sediments should account for the diagenetic transformations of reactive P and explain the deviation of the C/P_{org} from the Redfield ratio assumed for marine organic matter (106:1) [*Anderson and Delaney*, 2001]. The C/P_{reac} ratio generally shows values lower than the Redfield ratio, averaging 20, as it is observed for sediments with relatively low C_{org} contents (<2%) [see *Anderson and Delaney*, 2001]. Such low values indicate that reactive phosphorus exceeds organic carbon. The contrasting behavior of C/P_{org} and C/P_{reac} during part of the studied sequence, especially stage 5 (Figure 10), when C/P_{org} increases while C/P_{reac} shows low values, may be interpreted as another evidence of a ''phase switching'' between organic and authigenic P. Although part of the original organic carbon has also been oxidized and lost, it is clear that organic phosphorus cannot account alone for the C/P_{reac} values, and an alternative source of dissolved reactive phosphorus needs to be considered. *Schenau et al.* [2000] have demonstrated that fish debris dissolution constitutes an additional and important source of dissolved reactive phosphorus for modern sediments of the Oman margin. C/P_{reac} values ranging between 30 and 60 are observed only between 45 and 35 ka and between 20 and ka, when also the C/P_{org} ratio presents high numbers (Figure 10). These two peaks could be explained by either a reduced phosphorus input to the system, or an increased C preservation in the sediments relative to P, or a reduced phosphorus retention in the sediments, compared to interglacial periods. During stage 3, the co-occurrence of relatively high $\delta^{15}N$ with the peak in the C/P_{reac} ratio (Figures 9 and 10), may indicate low oxygen content of the bottom waters, which likely prompted the release of dissolved phosphorus to the water column. This is true especially if we assume that organic P regeneration from organic matter is enhanced under low oxygen conditions relative to oxic bottom waters [*Ingall and Jahnke*, 1994]. In fact, enhanced regeneration of nitrogen and phosphorus during anaerobic oxidation of the organic matter has been documented in sediments from the northeastern Arabian Sea [*Lueckge et al.*, 1999]. During the LGM, low oxygen levels may have persisted [see *Sirocko et al.*, 2000] and promoted the release of dissolved reactive P.

4. Implications

[40] The results obtained from the multiproxy study of sediments from the Oman margin have revealed three different situations as the response to changed monsoon strength, sea level, and oceanic circulation for the last 140,000 years (Figure 11).

[41] During full interglacial periods (i.e., lower part of stage 5 and stage 1; Figure 11a), characterized by high sea level stands and strong summer monsoon activity, the Oman margin showed high biological production rates, connected to increased upwelling intensity. *G. bulloides* % (upwelling indicator) and carbonate content are high. The enhanced upwelling and the input of intermediate waters from the Red Sea contributed to maintain high nutrient levels. However, low organic matter accumulation rates seem to indicate that productivity and/or preservation were not enhanced compared to glacial periods.

[42] Oxygen levels were probably low, as expected in high productivity regions and with the presence of an OMZ, but it is not clear from our data (see $\delta^{15}N$, OI) if severe anoxic conditions developed. In fact, increased and intense upwelling could have possibly brought oxygen-rich waters from below the OMZ to shallower depths, decreasing therefore its intensity [*Prell and Niitsuma*, 1989]. Low $\delta^{15}N$ during interglacial 5 could indicate effective nitrogen fixation by cyanobacteria, if nutrients other than nitrogen were provided to surface waters. Extensive oxidation of organic matter (as indicated by C/P_{org} and OI, Figures 9 and 10) and dissolution of fish debris regenerated high quantities of dissolved P that could in part precipitate as authigenic P and in part be upwelled to the surface water, enhancing productivity.

[43] Low detrital contents of the sediments during stage 5 are interpreted as the result of prevailing humid conditions on the mainland [*Burns et al.*, 1998]. The ITCZ (Intertropical Convergence Zone) was, in fact, located inside the Arabian peninsula and northwesterly winds could not reach the investigated site. Apparently, the increased humidity did not develop a coastal riverine system, which could enhance nutrient and dissolved phosphorus input. But during warm interglacials a continental input of nutrient to the ocean is not likely to have occurred. There is no evidence of any kind of terrestrial contribution to the organic pool, and proxies, such as the HI index (Figure 8), indicate an autochthonous origin of the organic matter.

[44] During glacials stages 4 and 2, and during stage 3, the ITCZ shifted southward and arid conditions prevailed on land, promoting eolian uptake of material (Figures 11b and 11c) [*Burns et al.*, 1998]. Northwesterlies, now blowing more southwardly, along with persistent and stronger northeasterlies contributed to high detrital input from the

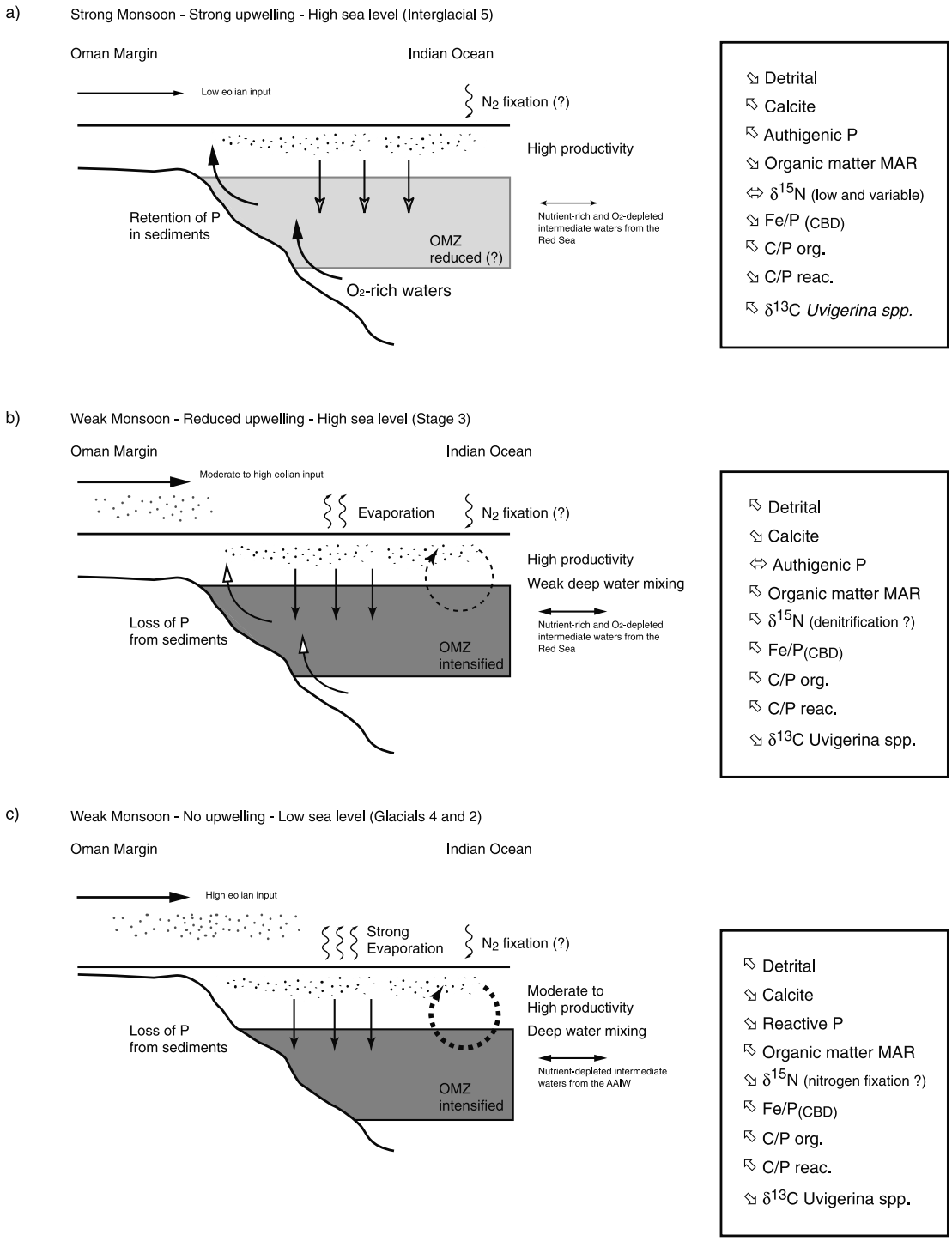

Figure 11. Schematic representations of the oceanographic and climatic situation during the last 140,000 years along the Oman margin. Generally low nitrogen stable isotopes are interpreted as indicating nitrogen fixation in surface waters, in response to quasi-persistent high nutrient levels. (a) During full interglacial periods biological production rates are relatively high, due to increased upwelling intensity and input of nutrient-rich waters from the Red Sea. Productivity and/or preservation of OM were not enhanced compared to glacial periods. (b) Relatively higher nitrogen stable isotopes values might reflect denitrification. Deep water mixing might be responsible for providing nutrients to surface waters, especially during weak summer monsoon periods. (c) The enhanced eolian input introduced high amounts of nutrients (e.g., Fe and possibly P, see text), which sustained productivity. Changes in sea level deeply influenced the circulation patters of the region.

continent, as indicated by all the detrital indices (i.e., quartz, phyllosilicates, this study, as well as Ti/Al, Fe/Ti) [*Shimmield and Mowbray*, 1991]. Despite their increased strength, winter monsoons were too weak to produce any substantial upwelling [*Madhupratap et al.*, 1996]. But several proxies, such as organic matter, nitrogen stable isotopes (this study) and $\delta^{13}C$ *Uvigerina spp.* (Figure 9) [*Zahn and Pedersen*, 1991] clearly point out that productivity and burial of organic matter were enhanced. Winter monsoon dryness has been called as the factor causing high nutrient content; in fact, during winter time, sinking of cooler and denser surface waters provoked an upward flux of deep and nutrient-rich waters [*Madhupratap et al.*, 1996].

[45] Stage 3 is characterized by a reduced summer monsoon-induced upwelling, and generally arid conditions were persistent on the continent [*Burns et al.*, 1998]. The high sea level fostered the input of oxygen-depleted intermediate waters from the Red Sea and persistent winter monsoons introduced high amounts of detrital material and micronutrients, such as iron (Figures 4, 5 and 6). One question to be answered here is whether reactive phosphorus concentrations in surface waters were high during glacial periods (stages 4-2). The indications we get from our data suggest that regeneration of dissolved phosphorus might have happened, and that part of this phosphorus might have been brought to surface waters. But more than that, it is reasonable that the input of reactive P from the continent might have been enhanced. In fact, ''continental'' Fe oxyhydroxides, an important component of eolian dust, which increased during glacials (Figure 7), generally bear considerable amounts of phosphorus adsorbed on their surfaces. Once in the ocean, photochemical reactions in the surface waters (i.e., photoreduction) [*Johnson et al.*, 1994] may dissolve part of the Fe oxyhydroxides, and, hence, liberate also the associated phosphorus (K. C. Ruttenberg, personal communication, 2002). This process, along with the above mentioned evaporation-induced mixing process, might have been responsible for maintaining high nutrients levels along the Oman margin (Figures 11b and 11c).

[46] Weaker upwelling along with persistent high productivity, probably enhanced the intensity of the OMZ, and stronger depletion of oxygen in bottom waters led to high organic matter accumulation and preservation, as indicated by C_{org} MAR and OI (Figures 4 and 9). Nitrogen isotopes are highest and show strong correlation with organic matter, possibly an indication of denitrification. Degradation of organic matter regenerated high amounts of dissolved reactive phosphorus, while organic carbon was preserved in the sediments [*Ingall and Jahnke*, 1994]. However, the extension of the OMZ during stage 3 and the consequent oxygen demand probably provoked unfavorable conditions to authigenic P precipitation, as indicated by low values of authigenic P, and high C/P_{reac} ratios (Figures 6 and 10). A diagenetic model developed for phosphorus cycling and applied to results from box cores from the Oman margin [*Slomp et al.*, 1996a; *Schenau et al.*, 2000], confirms that without bioturbation and in intense oxygen-depleted waters, reactive phosphorus is easily regenerated at the water-sediment interface and can re-enter the water column. A direct correlation among high sedimentation rates, low oxygen content, high organic carbon preservation and high phosphorus loss from the sediments might be forwarded for this period [*Colman and Holland*, 2000].

[47] During glacial stages 4 and 2, arid conditions on the continent [*Burns et al.*, 1998] allowed for high eolian input of detrital material and iron- (and phosphorus) containing dust. The well-crystallized iron oxides did not provide an efficient sink for dissolve P, which was probably not retained in the sediments. Glacial lowering of sea level reduced or even cut off the contribution from the Persian Gulf and the Red Sea, allowing waters from remote sources, possibly AAIW (Antarctic Intermediate Water) to spread northward (Figure 11c) [*Kallel et al.*, 1988].

[48] Glacial mass accumulation rates of organic carbon were high, especially during stage 2, promoting low oxygen conditions [*Sirocko et al.*, 2000]. Peaks in both C/P_{org} and C/P_{reac} indicate, indeed, a loss of dissolved P from the sediments, compared to interglacial periods (Figure 10). This implies that during glacial periods P release from the sediments was most likely enhanced and regenerated P, along with nutrients and micronutrients introduced from the mainland, could have sustained high rates of productivity.

5. Conclusions

[49] This multiproxy approach to the study of Site 724 allows for the explanation of different aspects of the climatic and oceanographic history of the Oman margin since interglacial 5.

[50] During the last 140,000 years, the Oman margin was characterized by an extremely complex situation, where regional and global processes were coupled and interacted. Changes in monsoon intensity, due to glacial-interglacial variations in insolation strength, did combine with different oceanic circulation modes, imposed by glacioeustatic changes in sea level, and both controlled sedimentation, nutrients distribution and primary production (Figure 11).

[51] Along with the other used proxies, the study of the different P phases stored in the Oman sediments brought important elements, because their variations are the product not only of the input from the mainland, but also of changes in physical and chemical conditions at the sea bottom, produced by changes in productivity, oceanic circulation and glacioeustatism. During the last 140,000 years the overall flux of P to the Oman margin sediments seemed not to have changed significantly; despite this, its redistribution and regeneration, both controlled by changed conditions in the sediments, as deduced by comparing reactive phosphorus and organic carbon records, have certainly played an important role in sustaining productivity.

[52] During full interglacial stages (stages 5 and 1), with strong summer monsoon inducing intense upwelling, productivity was sustained by the contribution of renewed nutrients from below the thermocline. Preservation was not enhanced because of persisting oxic or slightly suboxic conditions at the water-sediment interface. Phosphorus was regenerated during respiration of OM, and could partially precipitate as CFA. During glacial periods (stages 4-2), P was preferentially regenerated and rediffused to the water

column, because of low oxygen conditions in the bottom waters. Deep vertical mixing, along with eolian input of nutrients, helped in providing the renewed nutrients to the euphotic zone, sustaining productivity.

[53] From this study, productivity along the Oman margin emerges to be a quasi-persistent phenomenon across glacial and interglacial stages, and seems to be controlled both by summer monsoon-induced upwelling and winter monsoon-induced deep vertical mixing. This has certainly important implications on the local and global carbon budget, especially on glacial-interglacial timescales. The hypothesis of high productivity along the Oman margin also during glacial periods could redefine the role of monsoon regions in controlling and enhancing carbon dioxide drawdown from the atmosphere into the ocean and in maintaining low CO_2 concentrations during glacials.

[54] **Acknowledgments.** The authors thank Sébastien Ryser and José Richard for their help in the laboratory. Special thanks to Hilary Paul for her help in processing samples for $\delta^{15}N$ analysis. We gratefully acknowledge J. Ondrus and S. Pierrehumbert of the SCPE-laboratory of the canton of Neuchâtel for ICP-AES. The authors also thank Caroline Slomp and Sylvain Huon for their remarks on a early version of the paper, and Michael Arthur and two anonymous reviewers for their comments and helpful suggestions. This research used samples and/or data provided by the Ocean Drilling Program (ODP). ODP is sponsored by the U.S. National Science Foundation (NSF) and participating countries under management of Joint Oceanographic Institutions (JOI), Inc. Financial support to F.T. was provided by the University of Neuchâtel, and by the Swiss National Science Foundation. Analytical facilities were provided by the Geological Institute of Neuchâtel and the ETH Stable Isotope Laboratory of Zürich.

References

Altabet, M. A., D. W. Murray, and W. L. Prell, Climatically linked oscillations in Arabian Sea denitrification over the past 1 m.y.: Implications for the marine N cycle, *Paleoceanography*, *14*(6), 732–743, 1999.

Anderson, D. M., and W. L. Prell, Coastal upwelling gradient during the Late Pleistocene, *Proc. ODP Sci. Res.*, *117*, 265–273, 1991.

Anderson, L. D., and M. L. Delaney, Sequential extraction and analysis of phosphorus in marine sediments: Streamlining of the SEDEX procedure, *Limnol. Oceanogr.*, *45*(2), 509–515, 2000.

Anderson, L. D., and M. L. Delaney, Carbon to phosphorus ratios in sediments: Implications for nutrient cycling, *Global Biogeochem. Cycles*, *15*(1), 65–79, 2001.

Bertrand, P., E. Lallier-Verges, and H. Grall, Organic petrology of Neogene sediments from North Indian Ocean (Leg 117): Amount, type, and preservation of organic matter, *Proc. ODP Sci. Res.*, *117*, 587–594, 1991.

Bethoux, J. P., Red Sea geochemical budgets and exchanges with the Indian Ocean, *Mar. Chem.*, *24*, 83–92, 1988.

Broecker, W. S., and T.-H. Peng, *Tracers in the Sea*, Lamont-Doherty Geol. Observ., Palisades, N. Y., 1982.

Burns, S. J., A. Matter, N. Frank, and A. Mangini, Speleothem-based paleoclimate record from northern Oman, *Geology*, *26*(6), 499–502, 1998.

Canfield, E. D., Organic matter oxydation in marine sediments, in *Interactions of C, N, P and S Biogeochemical Cycles and Global Change*, edited by R. Wollast, F. T. MacKenzie, and L. Chou, pp. 333–363, Springer-Verlag, New York, 1993.

Capone, D. G., J. P. Zehr, H. W. Paerl, B. Bergman, and E. J. Carpenter, *Trichodesmium*, a globally significant marine cyanobacteria, *Science*, *276*, 1221–1229, 1997.

Chavez, F. P., and J. R. Toggweiler, Physical estimates of global new production: The upwelling contribution, in *Upwelling in the Ocean: Modern Processes and Ancient Records*, edited by C. P. Summerhayes et al., pp. 313–320, 1995.

Colman, A. S., and H. D. Holland, The global diagenetic flux of phosphorus from marine sediments to the oceans: Redox sensitivity and the control of atmospheric oxygen levels, in *Marine Authigenesis: From Global to Microbial*, pp. 53–75, Soc. for Sediment. Geol., Tulsa, Okla., 2000.

Compton, J., D. Mallison, C. R. Glenn, G. Filippelli, K. Föllmi, G. Shields, and Y. Zanin, Variations in the global phosphorus cycle, in *Marine Authigenesis: From Global to Microbial*, pp. 21–33, Soc. for Sediment. Geol., Tulsa, Okla., 2000.

Debrabant, P., L. A. Krissek, A. Bouquillon, and H. Chamley, Clay mineralogy of Neogene sediments of the western Arabian Sea: Mineral abundances and paleoenvironmental implications, *Proc. ODP Sci. Res.*, *117*, 183–196, 1991.

Delaney, M. L., Phosphorus accumulation in marine sediments and the oceanic phosphorus cycle, *Global Biogeochem. Cycles*, *12*(4), 563–572, 1998.

Espitalié, J., G. Deroo, and F. Marquis, La pyrolyse Rock-Eval et ses applications—III partie, *Rev. Inst. Fr. Pet.*, *41*(1), 73–89, 1986.

Föllmi, K. B., The phosphorus cycle, phosphogenesis and marine phosphate-rich deposits, *Earth Sci. Rev.*, *40*, 55–124, 1996.

Froelich, P. N., M. L. Bender, N. A. Luedtke, G. R. Heath, and T. DeVries, The marine phosphorus cycle, *Am.J. Sci.*, *282*(4), 474–511, 1982.

Glenn, C. R., Pore water, petrologic and stable carbon isotopic data bearing on the origin of modern Peru margin phosphorites and associated authigenic phases, in *Neogene to Modern Phosphorites*, edited by S. R. Riggs and W. C. Burnett, pp. 46–61, Cambridge Univ. Press, New York, 1990.

Goddéris, Y., and L. M. François, The Cenozoic evolution of the strontium and carbon cycles: Relative importance of continental erosion and mantle exchanges, *Chem. Geol.*, *126*, 169–190, 1995.

Haug, G. H., T. F. Pedersen, D. M. Sigman, S. E. Calvert, B. Nielsen, and L. C. Peterson, Glacial/interglacial variations in production and nitrogen fixation in the Cariaco Basin during the last 580 kyr, *Paleoceanography*, *13*(5), 427–432, 1998.

Hedges, J. I., W. A. Clark, and G. L. Cowie, Organic matter sources to the water column and surficial sediments of a marine bay, *Limnol. Oceanogr.*, *33*, 1116–1136, 1988.

Heinze, C., E. Maier-Reimer, and K. Winn, Glacial pCO_2 reduction by the world ocean: Experiments with the Hamburg carbon cycle model, *Paleoceanography*, *6*(4), 395–430, 1991.

Imbrie, J., J. D. Hays, D. G. Martinson, A. McIntyre, A. C. Mix, J. J. Morley, N. G. Pisias, W. L. Prell, and N. J. Shackleton, The orbital theory of Pleistocene climate: Support from a revised chronology of the marine delta 18O record, in *Milankovitch and Climate*, edited by A. Berger et al., pp. 269–305, D. Reidel, Norwell, Mass., 1984.

Ingall, E., and R. Jahnke, Evidence for enhanced phosphorus regeneration from marine sediments overlain by oxygen depleted waters, *Geochim. Cosmochim. Acta*, *58*(11), 271–275, 1994.

Jarvis, I., et al., Phosphorite geochemistry: state-of-art and environmental concerns, *Eclogae Geol. Helv.*, *87*(3), 643–700, 1994.

Johnson, K. S., K. H. Coale, V. A. Elrod, and N. W. Tindale, Iron photochemistry in seawater from the equatorial Pacific, *Mar. Chem.*, *46*, 319–334, 1994.

Kallel, N., L. D. Labeyrie, A. Juillet-Leclerc, and J.-C. Duplessy, A deep hydrological front between intermediate and deep-water masses in the glacial Indian Ocean, *Nature*, *333*, 651–655, 1988.

Kenig, F., B. N. Popp, J. M. Hayes, and R. Summons, An isotopic biogeochemical study of the Oxford Clay formation, Jurassic, UK, *J. Geol. Soc. London*, *151*, 139–152, 1994.

Krajewski, K. P., et al., Biological processes and apatite formation in sedimentary environments, *Eclogae Geol. Helv.*, *87*(3), 701–745, 1994.

Krissek, L. A., and S. C. Clemens, Mineralogic variations in a Pleistocene high-resolution eolian record from the Owen Ridge, western Arabian Sea (Site 722): Implications for sediment source conditions and monsoon history, *Proc. ODP Sci. Res.*, *117*, 197–211, 1991.

Krissek, L. A., and S. C. Clemens, Evidence for aridity-driven dust flux to the northwest Arabian Sea and for decoupling of the dust and upwelling system, in *Upwelling Systems: Evolution Since the Early Miocene*, edited by C. P. Summerhayes, W. L. Prell, and K. C. Emeis, pp. 359–378, Geol. Soc., London, 1992.

Kübler, B., Dosage quantitatif des minéraux majeurs des roches sédimentaires par diffraction X, *Cah. de l'Inst. de Géol. de Neuchâtel, Sér. ADX*, Inst. of Geol., Univ. of Neuchatel, Switzerland, 1987.

Lafargue, E., J. Espitalié, F. Marquis, and D. Pillot, Rock Eval 6 applications in hydrocarbon exploration, production and in soil contamination studies, in *Latin American Congress on Organic Geochemistry, ALAGO Spec. Publ.*, edited by M. E. Gomez Luna and A. M. Cortés, pp. 364–366, Cancun, 1996.

Langford, F. F., and M.-M. Blanc-Valleron, Interpreting rock-Eval pyrolysis data using graphs of pyrolizable hydrocarbons versus total organic carbon, *Am. Assoc. Pet. Geol.*, *74*(6), 799–804, 1990.

Lohse, L., R. T. Kloosterhuis, H. C. de Stigter, W. Helder, W. van Raaphorst, and T. C. E. van Weering, Carbonate removal by acidification causes loss of nitrogenous compounds in continental margin sediments, *Mar. Chem.*, *69*, 193–201, 2000.

Lucotte, M., A. Mucci, C. Hillaire-Marcel, and S. Tran, Early diagenetic processes in deep Labrador Sea sediments: Reactive and nonreactive iron and phosphorus, *Can. J. Earth Sci.*, *31*, 14–27, 1994.

Lueckge, A., M. Ercegovac, H. Strauss, and R. Littke, Early diagenetic alteration of organic matter by sulfate reduction in Quaternary sediments from the northeastern Arabian Sea, *Mar. Geol.*, *158*(1–4), 1–137, 1999.

Madhupratap, M., S. Prasanna Kumar, P. M. A. Bhattathiri, M. Dileep Kumar, S. Raghukumar, K. K. C. Nair, and N. Ramaiah, Mechanism of the biological response to winter cooling in the northeastern Arabian Sea, *Nature*, *384*, 549–552, 1996.

Murray, D. W., and W. L. Prell, Pliocene to Pleistocene variations in calcium carbonate, organic carbon, and opal on the Owen Ridge, northern Arabian sea, *Proc. ODP Sci. Res.*, *117*, 343–363, 1991.

Muzuka, A. N. N., S. A. Macko, and T. F. Pedersen, Stable carbon and nitrogen isotope compositions of organic matter from Sites 724 and 725, Oman Margin, *Proc. ODP Sci. Res.*, *117*, 571–586, 1991.

Prell, W. L., Monsoonal climate of the Arabian Sea during late Quaternary: A response to changing solar radiation, in *Milankovitch and Climate*, edited by A. L. Berger et al., pp. 349–366, D. Reidel, Norwell, Mass., 1984.

Prell, W. L., and J. E. Kutzbach, Monsoon variability over the past 150,000 years, *J. Geophys. Res.*, *92*(D7), 8411–8425, 1987.

Prell, W. L., and N. Niitsuma, *Proceedings of the Ocean Drilling Program*, *Initial Report 117*, pp. 5–10, Ocean Drill. Prog., College Station, Tex., 1989.

Prell, W. L., et al., Site 724 proceedings of the Ocean Drilling Program, Oman margin/Neogene package, covering Leg 117 of the cruises of the drilling vessel JOIDES Resolution, Port Louis, Mauritius, to Port Louis, Mauritius, sites 720–731, 19 August 1987–17 October 1987, *Proc. Ocean Drill. Prog. Part A, Init. Rep.*, *117*, 385–417, 1989.

Prell, W. L., D. W. Murray, S. C. Clemens, and D. M. Anderson, Evolution and variability of the Indian Ocean summer monsoon: Evidence from the western Arabian Sea Drilling Program, in *The Indian Ocean: A Synthesis of Results From the Ocean Drilling Program*, edited by R. A. Duncan, pp. 447–469, AGU, Washington, D. C., 1992.

Raymo, M. E., The Himalayas, organic carbon burial and climate in the Miocene, *Paleoceanography*, *9*(3), 399–404, 1994.

Reichart, G. J., L. J. Lourens, and W. J. Zachariasse, Temporal variability in the northern Arabian Sea Oxygen Minimum Zone (OMZ) during the last 225,000 years, *Paleoceanography*, *13*(6), 607–621, 1998.

Ruttenberg, K. C., Development of a sequential extraction method for different forms of phosphorus in marine sediments, *Limnol. Oceanogr.*, *37*(7), 1460–1482, 1992.

Ruttenberg, K. C., and M. A. Gõni, Phosphorus distribution, C:N:P ratios, and $\delta^{13}C_{oc}$ in arctic, temperate, and tropical coastal sediments: Tools for characterizing bulk sedimentary organic matter, *Mar. Geol.*, *139*, 123–145, 1997.

Schenau, S. J., C. P. Slomp, and G. J. De Lange, Phosphogenesis and active phosphorite formation in sediments from the Arabian Sea oxygen minimum zone, *Mar. Geol.*, *169*(1–2), 1–20, 2000.

Sherwood, B. A., S. L. Sager, and H. D. Holland, Phosphorus in foraminiferal sediments from North Atlantic Ridge cores and in pure limestones, *Geochim. Cosmochim. Acta*, *51*, 1861–1886, 1987.

Shimmield, G. B., and S. R. Mowbray, The inorganic geochemical record of the northwest Arabian Sea: A history of productivity variation over the last 400 k.y. from sites 722 and 724, *Proc. OPD Sci. Res.*, *117*, 409–429, 1991.

Sirocko, F., Accumulation of eolian sediments in the northern Indian Ocean; record of the climatic history of Arabia and India, Ph.D. thesis, 185 pp., Geol. Paleontol. Inst. and Mus., Christian Albrechts Univ., Kiel, Germany, 1989.

Sirocko, F., M. Sarnthein, H. Erlenkeuser, H. Lange, M. Arnold, and J. C. Duplessy, Century-scale events in monsoonal climate over the past 24,000 years, *Nature*, *364*, 322–324, 1993.

Sirocko, F., D. Garbe-Schönberg, and C. Devey, Processes controlling trace elements geochemistry of Arabian Sea sediments during the last 25,000 years, *Global Planet. Change*, *26*, 217–303, 2000.

Slomp, C. P., Early diagenesis of phosphorus in continental margin sediments, Ph.D. thesis, Den Burg, Texel, Netherlands, 1997.

Slomp, C. P., E. H. G. Epping, W. Helder, and W. van Raaphorst, A key role of iron-bound phosphorus in authigenic apatite formation in North Atlantic continental platform sediments, *J. Mar. Res.*, *54*, 1179–1205, 1996a.

Slomp, C. P., S. J. Van der Gaast, and W. Van Raaphorst, Phosphorus binding by poorly crystalline iron oxides in North Sea sediments, *Mar. Chem.*, *52*, 55–73, 1996b.

Webster, P. J., V. O. Magana, T. N. Palmer, J. Shukla, R. A. Tomas, M. Yanai, and T. Yasunari, Monsoons: Processes, predictability, and the prospects for prediction, *J. Geophys. Res.*, *103*(C7), 14,451–14,510, 1998.

Weedon, G. P., and G. B. Shimmield, Late Pleistocene upwelling and productivity variations in the northwest Indian Ocean deduced from spectral analyses of geochemical data from sites 722 and 724, *Proc. ODP Sci. Res.*, *117*, 431–443, 1991.

Zahn, R., and T. F. Pedersen, Late Pleistocene evolution of surface and mid-depth hydrography at the Oman margin: Planktonic and benthic isotope records at Site 724, *Proc. ODP Sci. Res.*, *117*, 291–308, 1991.

Zahn, R., K. Winn, and M. Sarnthein, Benthic foraminiferal $\delta^{13}C$ and accumulation rates of organic carbon: Uvigerina Peregrina group and Cibicidoides Wuellerstorfi, *Paleoceanography*, *1*(1), 27–42, 1986.

T. Adatte, K. B. Föllmi, and P. Stenmann, Institut de Géologie, Université de Neuchâtel, Rue Emile-Argand 11, CH-2007 Neuchâtel, Switzerland. (Thierry.adatte@unine.ch; karl.foellmi@unine.ch; philipp.steinmann@unine.ch)

S. M. Bernasconi, Geologisches Institut, ETH-Zentrum, Sonneggstrasse 5, CH-8092 Zürich, Switzerland. (stefano@erdw.ethz.ch)

F. Tamburini, Woods Hole Oceanographic Institution, Marine Geology and Chemistry Department, Mail Stop #8, Woods Hole, MA 02543, USA. (ftamburini@whoi.edu)